Exploring the Kuramoto model of coupled oscillators in minimally cognitive evolutionary robotics tasks

Renan C. Moioli, Patricia A. Vargas and Phil Husbands

Abstract— **This work is the first attempt to investigate the neural dynamics of a simulated robotic agent engaged in minimally cognitive tasks by employing evolved instances of the Kuramoto model of coupled oscillators as its nervous system. The main objectives are to shed new light into the role of neuronal synchronization and phase towards the generation of cognitive behaviours and to initiate an investigation on the efficacy of such systems as practical robot controllers. The first experiment is an active categorical perception task in which the robot has to discriminate between moving circles and squares. In the second task, the robotic agent has to approach moving circles with both normal and inverted vision thus adapting to both scenarios. These tasks were chosen for being considered as benchmarks in the evolutionary robotics and adaptive behaviour communities. The results obtained indicate the feasibility of the framework in the analysis and generation of embodied cognitive behaviours.**

I. Introduction

Oscillatory phenomena have been formally studied since at least the 1650s when Christiaan Huygens invented the pendulum clock, leading to his analysis of pendulum motion and his later development of the wave theory of light. Since then it has been noticed that many events in nature can be understood in terms of their oscillatory properties, with examples ranging from firefly blinking patterns [1] to the synchronisation of multiple laser beams [2]. Following the birth of modern neuroscience at the turn of the last century, it wasn't long before researchers started looking at neuronal dynamics from an oscillatory perspective [3]. The consensus nowadays is that cognitive processes have a close non-trivial relationship to neuronal rhythms and oscillations [4]. The importance of considering temporal relations among groups of neurons (temporal coding), either by external influences or sustained by internal mechanisms, has been stressed by various researchers in recent years [5, 6, 7, 8].

According to Varela et al. [9] it is essential to investigate the temporal dynamics of neural networks in order to understand the emergence and integration of neuronal assemblies by means of synchronisation. These dynamic assemblies, which are related to large-scale neuronal integration, can influence every cognitive act an agent might eventually perform. In studying these temporal dynamics, Varela and collaborators opted to focus on the phase relationships of brain signals, mainly because these contain a great deal of information on the temporal structure of neural signals, particularly those relating to the underlying mechanism for brain integration. Other authors have emphasized the relationship between phase information and memory formation and retrieval [10, 11, 12].

It is now well established that robotics models are highly suited to capture essential elements of the brain/body/environment interactions that underlie the generation of behaviour, in a way that studies of disembodied neuronal dynamics cannot achieve [13, 14]. Evolutionary robotics has an important role in this context as it allows the exploration of classes of mechanisms, and the automatic creation of working models when there are insufficient details to fully specify a system in advance. Hence it has been recognized as a useful tool in investigating biological hypotheses [15, 16, 17]. Although there has been much work on coupled oscillator based control of complex motor behaviours, particularly locomotion [18], to date there has been very little research on the wider issues of neuronal synchronisation and phase information in the generation of embodied cognitive behaviours. Hence the work presented in this paper sets out to explore the neural dynamics of a simulated robotic agent, employing a network of oscillators as its nervous system, engaged in minimally cognitive tasks, i.e. tasks that are simple enough to allow detailed analysis and yet are complex enough to motivate some kind of cognitive interest. The work has dual aims: both to shed new light on the role of neuronal synchronisation and phase in the generation of cognitive behaviours, and to begin investigating the efficacy of such systems as practical robotic controllers.

For the first time, we apply evolved instances of the Kuramoto model of coupled oscillators [19] to the generation of minimally cognitive behaviour, studying two tasks. The first is an active categorical perception task [13, 20, 21] in which the robot has to discriminate between moving circles and squares. In the second task, the robotic agent has to approach moving circles with both normal and inverted vision, adapting to both conditions. Even though these tasks don't strictly require a network of coupled oscillators to be solved, they have been chosen for being regarded as benchmarks in the evolutionary robotics and adaptive behaviour communities [22, 13, 21, 20].

The rationale behind the choice of the Kuramoto is that it describes the phase evolution of a set of connected oscillators and with some adjustments can be associated with groups of neurons firing at a periodic rate [23]. Therefore, instead of focusing on single neuron activations, the model resembles the behaviour of groups of neurons. By using the phase

Renan C. Moioli and Phil Husbands are with the Centre for Computational Neuroscience and Robotics (CCNR), Department of Informatics, University of Sussex, Falmer, Brighton, BN1 9QH, United Kingdom, (email: {r.moioli, p.husbands}@sussex.ac.uk). Patricia A. Vargas is with the School of Maths and Computer Science, Heriot-Watt University, Edinburgh, Scotland, EH14 4AS, United Kingdom, (email: p.a.vargas@hw.ac.uk)

dynamics as the central feature of the model, the focus is on short-term temporal activity, which has been previously shown to be successful in pattern recognition tasks [24, 2]. Furthermore, the model allows for easy inspection of the phase and frequency of each of the elements, which makes it especially suitable for studying synchronisation of groups of oscillators [25], a key factor when analysing communication and information processing in neuronal assemblies [26, 27]. Izhikevich [11] shows that depending on changes in phase relationships caused by external/internal stimulus, neurons can reorganize and synchronize themselves with different neurons, thus changing their response without the need to change its synaptic weights. This points towards new kinds of behaviour generating mechanisms that are explored in the work presented here.

This paper is organized as follows: section II defines the Kuramoto model and its adaptation for use in our evolutionary robotics studies; section III describes the experiments and their implementation procedures; section IV shows the results and provides some analysis and section V presents the final discussion, conclusions and proposes further work.

II. The Kuramoto Model

Among many models proposed to study oscillatory behaviour, Winfree's model [28] is one of the most explored and has been applied to investigate large populations of biological oscillators (e.g. fireflies, crickets, circadian pacemaker cells and eventually neurons). The essence of his model is represented by a lattice of coupled oscillators, each with a possible different natural frequency drawn from some distribution, modulated according to a function that depicts their sensitivity to the phase in each other node. The Kuramoto model [19] is defined when this influence function from a node i to a node j assumes the form of $sin(\theta_j - \theta_i)$, where θ stands for the phase of the node.

Kuramoto observed that under certain conditions the influence function could be represented by the first term of its Fourier series, the rest of it being suppressed, hence the $sin(\theta_j - \theta_i)$ substitution. It has been widely investigated in the literature, with successful approaches ranging from superconductor's physics [29] to pattern recognition [2]. Some mathematical analysis can be carried on the Kuramoto model, but its dynamics can easily scale up in complexity. The model has the form of Equation 1. It can present a large variety of synchronisation patterns and can be adapted to many different scenarios. However, it is considered to be intractable analytically.

$$\frac{d\theta_i}{dt} = \omega_i + \frac{k}{n}\sum_{j=1}^{n} sin(\theta_j - \theta_i) \tag{1}$$

where: θ_i is the phase of the *i*th oscillator, ω_i is the natural frequency of the *i*th oscillator, k is the coupling factor between nodes and n is the total number of oscillators.

Basically, if the frequency of any two given nodes i and j $(i, j = 1, 2...n)$ are equal, i.e. $d\theta_i - d\theta_j = 0$ or $\theta_i - \theta_j = constant$, the model is said to be globally synchronized.

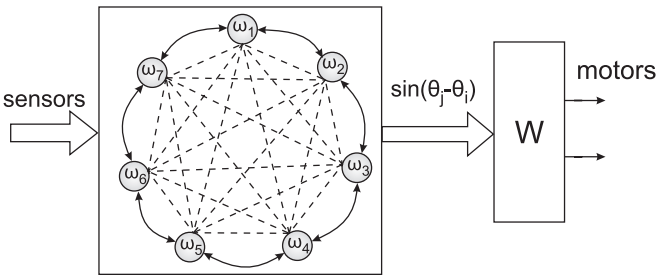

Fig. 1. Framework for application in evolutionary robotics. The oscillatory network is represented by a set of nodes connected by a thick line, in the case of the ring topology, or by dashed lines, in the case of the fully connected topology.

It is possible to calculate a synchronisation index, which would give a better idea on how synchronized the set of oscillators are [19]. Consider Equation 2, where r stands for the synchronisation index (1 meaning high synchronisation, 0 meaning incoherent oscillatory behaviour) and ψ stands for the mean phase of the system.

$$re^{i\psi} = \frac{1}{n}\sum_{j=1}^{n} e^{i\theta_j} \tag{2}$$

The Kuramoto model presents a series of properties that makes it suitable for the study of different types of synchronisation problems. Our work focuses on a particular property known as partial synchronism. Consider a network composed of 4 nodes, where each node is connected to its immediately two neighbours in a shape similar to a ring. Depending on the coupling factor k and the natural frequency w_i of each node, the network can present a global synchronous behaviour. Monteiro et al. [30] showed that by changing the frequency of one node the resultant network may exhibit partial synchronism, i.e., some of the nodes become synchronized while other nodes are not. Moreover, the oscillatory behaviour of one node can be influenced by another node in the network not necessarily connected to it.

The importance of this property in mimicking brain related dynamics relies in the fact that different neuronal blocks could synchronize and influence other blocks, and in consequence different cortical areas could flexibly establish communication channels depending on their temporal activity. This is in agreement with some recent findings in neuroscience [4], reinforcing the feasibility of applying the Kuramoto model to study cognitive processes.

A. Framework for application in evolutionary robotics

The model studied here is inspired by the aforementioned Kuramoto model, with some modifications made to it so that it could be applied to control a simulated robotic agent.

The framework is composed of a set of oscillators, connected in two possible ways: to its immediately two neighbours, giving the structure the shape of a ring (see Figure 1), or fully connected. In his original work, Kuramoto suggested a fully connected set-up, but other structures, including the ring shaped one, have been studied and proven to have a

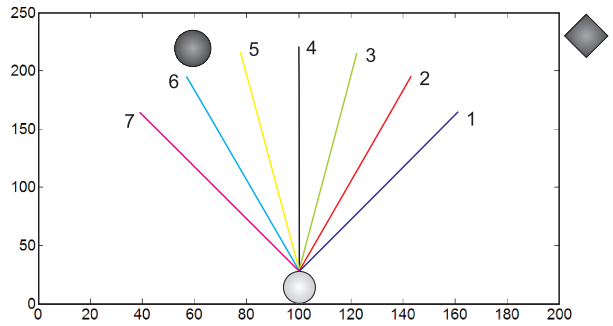

Fig. 2. Experiments 1 and 2 scenario. The agent (gray circle in the bottom) has to catch falling circles and avoid squares in Task 1 and catch falling circles with normal and inverted vision in Task 2. The robotic agent has 7 ray sensors, symmetrically displaced with relation to the central ray in intervals of $\pm pi/12$ radians, and two motors that can move it horizontally.

direct influence over the synchronisation properties of the model [31, 23, 32].

In our approach, the frequency of each node is the result of the sum of its natural frequency of oscillation, w_i, with the value of the sensory input related to that node, scaled by a factor z_i. The natural frequency w_i could be associated to the natural firing rate of a neuron or a group of neurons, and the sensory inputs mediated by z_i would alter its oscillatory behaviour according to the environmental context, improving the flexibility of the model to study cognitive processes and its neural correlates [23].

At each iteration the phase differences from a given node in relation to all other nodes it is connected to are calculated according to Equation 3. Based on the approach suggested by Schmidhuber et al. [33], the output of the network is given by the sine of the aforementioned phase differences linearly combined by the output weight matrix W. The sine function aims at reducing the phase differences instabilities caused by the phase resetting of each oscillator when it exceeds 2π. Therefore, there are n inputs to n correspondent nodes in the network, with $C_{n,2}$ phase differences being multiplied by a $C_{n,2} \times o$ matrix W, where o is the number of outputs.

$$\frac{d\theta_i}{dt} = (\omega_i + z_i I(t)) + k \sum_{j \in C_i} sin(\theta_j - \theta_i) \qquad (3)$$

where C_i is the set of nodes connected to node i.

In this way, the overall behaviour of the network will be dictated by the phase dynamics and the environmental input to the robotic agent. It is important to stress that, as shown in the previous section, nodes that are not directly connected can influence each other, depending on the frequency they have.

III. Methods

To investigate the framework presented in this paper, two tasks are studied, following the works of Beer [13] and Izquierdo [21].

In the first experiment an active categorical perception task is performed. It consists of a circular robotic agent able to move horizontally in a 250×200 rectangular environment (Figure 2). The robotic agent's body consists of 7 ray sensors, symmetrically displaced in relation to the central ray in intervals of $\pm pi/12$ radians, and two motors. An intersection between each sensory ray and an object reflects a reading between 0 and 10, 0 when the ray length is greater than 200 units and 10 when the ray length is 0. In all experiments, there is a saturation of the sensors (they are clamped) when their value is above 9. The robotic agent has to discriminate among circles and squares as they move from the top of the arena to the bottom (only one object at each trial), where the robotic agent is located. The square's diagonal, the robotic agent and the circle's radius measure 15 units. At the beginning of each trial, a circle or a square is dropped at the top of the scenario in a random horizontal position within a maximum of 50 units from the robotic agent, and moves vertically with a velocity of 3 units/step. The robotic agent, while being at the bottom, has to approach the circles and avoid the squares, adjusting its horizontal velocity accordingly.

The second experiment consists of an orientation task. In the same environmental set-up, the robotic agent has to adjust its horizontal position and catch circles, with normal and inverted vision. When submitted to visual inversion, sensory readings from an object at the right side of the agent are perceived by the agent's left set of sensors, and vice-versa. Therefore, different scenarios can cause similar sensory stimulus to the robotic agent thus requiring a different strategy depending on the current situation.

In this sense, the first task aims at investigating the performance of the proposed architecture in discriminating between two objects, whereas in the second task the robotic agent has to develop a strategy to overcome the disruption caused by the inversion of the visual field. In both scenarios, the focus will not be solely on the behaviour displayed by the robotic agent but also in the dynamics and synchronisation patterns of the proposed framework.

A genetic algorithm is used to determine the parameters of the system: the frequency of each node, $w_i \in [0, 10]$, the coupling factor $k \in [0, 5]$, the input weights $z_i \in [0, 3]$, the matrix $W_{C_{n,2},o}$ with elements in the interval $[-2, 2]$ and a motor output weight $s \in [0, 10]$, resulting in a genotype of length 58 for the tasks studied here.

The network's genotype consists of an array of integer variables lying in the range $[0, 999]$ (each variable occupies a gene locus), which are mapped to values determined by the range of their respective parameters. For all the experiments in this paper, the population size was 49, arranged in a 7×7 grid. A generation is defined as 100 breeding events and the evolutionary algorithm runs for a maximum of 100 generations. There are two mutation operators: the first operator is applied to 20% of the gene and produces a change at each locus by an amount within the $[-10, +10]$ range according to a normal distribution. The second mutation operator has a probability of 10% and is applied to 40% of the genotype. A randomly chosen gene locus is replaced

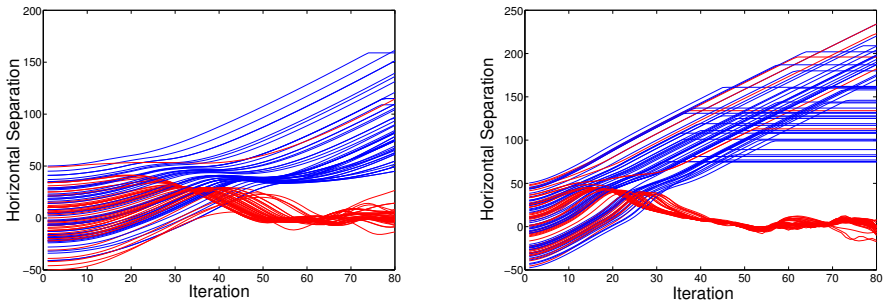

(a) (b)

Fig. 3. The generalization performance of the agent over 100 aleatory runs for the ring topology (a) and the fully connected topology (b). The red colour is related to the circle catch behaviour and the blue colour to the square avoidance behaviour. The plot illustrates the value of the horizontal separation of the agent and the object along 80 iterations.

with a new value within the $[0, 999]$ range in an uniform distribution. For further details about the genetic algorithm, the reader should refer to [34].

In the first experiment, an evolutionary run corresponds to 28 trials with randomly chosen objects (circles or squares), starting at an uniformly distributed horizontal offset in the interval of ± 50 units from the robotic agent. Fitness is defined as the robotic agent's ability to catch circles and avoid squares, and is calculated according to the following equation: $fitness = \sum_{i=1}^{N} if_i / \sum_{i=1}^{N} i$, where f_i is the ith value in a descending ordered vector $F_{1,N}$, and is given by $1-d_i$, in the case of a circle, or by d_i in the case of a square. d_i is the horizontal distance from the robotic agent to the object at the end of the ith trial (when the object reaches the bottom of the scenario), limited to 50 and normalized between 0 and 1. Therefore, a robotic agent with good fitness maximizes its distance from squares and minimizes its distance from circles. Notice that the fitness function pressures for a good performance in all trials in a given evolutionary run, instead of just averaging the performance of each trial, which could bias the mean fitness of a given robotic agent leading to a poor generalization behaviour.

In the second experiment, the evolutionary run corresponds to 20 trials with normal vision scheme followed by 20 trials with inverted vision. The circles are dropped at an uniformly distributed horizontal offset in the interval of ± 50 units from the robotic agent. Fitness for each part of the run is defined as above but considering just the circle catch scenario. The final fitness is calculated by averaging the fitness obtained under normal and inverted vision. Therefore, a robotic agent with good fitness minimizes its distance from circles, in both normal and inverted vision situations.

The next section presents the results, considering the highest fitness individual evolved for each proposed experiment.

IV. Results

A. Experiment 1

In the first experiment two network topologies were investigated, the ring topology and the fully connected topology. We will first focus on the ring topology moving to the analysis of the fully connected structure afterwards.

The training fitness of the best individual was 0.96 out of 1.00, and the generalization fitness over 100 random runs was 0.94, which resemble the results that are found in the literature [13, 20]. Figure 3(a) illustrates the generalization test.

In the first 10 iterations, the robotic agent remains practically motionless, as portrayed by the invariance of its horizontal separation in relation to the agent. The subsequent 10 iterations show that the behaviour of the robotic agent is very similar for both task scenarios, moving to one side of the falling object (in this case, moving to the right side of the object). From that iteration on, the discrimination process could be better observed. The robotic agent approaches the circles, centres itself in relation to the falling object, and continues to move to one side of the scenario to avoid the squares. This behaviour has been observed before in Izquierdo [21] for the same task but with a different neural controller architecture. One can attribute this behaviour to the asymmetric nature of the neural controller, i.e. the neural connection weights and other network parameters are not symmetric in relation to the robotic agent's body, which is the case of the controller studied in this paper. It is also pointed out that the strategy developed by asymmetric neural controllers are simpler than the ones developed by symmetrical ones, and that they were easier to evolve. However, that doesn't mean they are less capable of solving complex tasks. In fact, they achieved good performance levels in the tasks under analysis.

Figures 4 and 5 show the detailed behaviour of the robotic agent's internal and external dynamics for the two task developed behaviours (circle catch and square avoidance). Figure 4(a) shows the robotic agent's trajectory, the frequency of each node of the network and the phase dynamics, respectively. The upper part refers to the circle catch behaviour and the bottom part refers to the square avoidance behaviour.

It is possible to observe that the robotic agent successfully solves the task, moving close to circles and far from

squares. The oscillatory pattern of each node, as explained in Section II-A, depends on the sensory input and therefore varies according to the object being detected and the robotic agent's position in relation to the object. However, as it is going to be detailed in the next paragraph, the nodes can interact with each other and as a consequence the resultant global oscillatory behaviour is a combination of the perceived environment and the internal oscillatory state of the network, which means that the relevance of one node's response to an external stimulus will be modulated by the context established by the other nodes in the network.

The phase dynamics, as expressed by Equation 3, changes according to the frequency of each node and produces the different behaviours observed in the task. Notice that the network activity approaches the synchronized state in the square avoidance task (centre graphic of the bottom part of Figure 4(a)) as the robotic agent is receiving less stimulus from the environment. Also, the phase activity is smoother, when compared to the respective top part of the figure (circle catch behaviour). However, it is important to highlight that even without external stimulus there can be an oscillatory activity in the network. Lastly, the aforementioned synchronisation properties of the system are mainly dictated by the parameters of the oscillatory ring network (see Equation 3), such as the coupling factor k and the natural frequency of each node w_i [31, 32].

Figure 5 illustrates the detailed sensory input, the motor output, and the frequency of each node (upper two graphics for circle catch, bottom two for square avoidance, respectively). It is possible to observe, in both situations, that the oscillatory pattern of the network is not a direct product of the external stimulus and the node's natural frequency, but a composition with the other nodes frequency. For instance, in the top two graphics the sensory input tends to saturate as the robotic agent gets closer to the circle but the frequency of each node has a completely different behaviour. Notice the almost synchronized state of nodes 2 (red), 3 (green) and 7 (magenta) after iteration 70. This fact can also be observed between nodes 1 (black) and 5 (yellow), despite having different natural frequencies and not being all directly connected. Another interesting case happens near iteration 56: the frequency of node 6 (cyan) changes even without a direct environmental input to it, stressing the dependence of the overall network state in the determination of each node's frequency.

In the bottom two graphics, between iterations 30 and 50, even though sensors' 6 (cyan) and 7 (magenta) readings increase, the frequency of the correspondent nodes does not because they are also interacting with the other nodes. For instance, in the same time interval, node 1 (blue) has its frequency altered without receiving any external stimulus. The opposite happens in node 5 (yellow), between iterations 10 and 30, where in spite of the sensory reading the node's frequency remains almost unaltered.

Figure 6(a) shows the synchronisation index and the mean phase of the network, calculated using Equation 2. The overall behaviour of the network is almost equal until iteration 20, when a phase difference between both task scenarios (circle catch and square avoidance) starts to appear and the synchronisation index for the first case illustrates the lack of synchronisation observed in the previous figures.

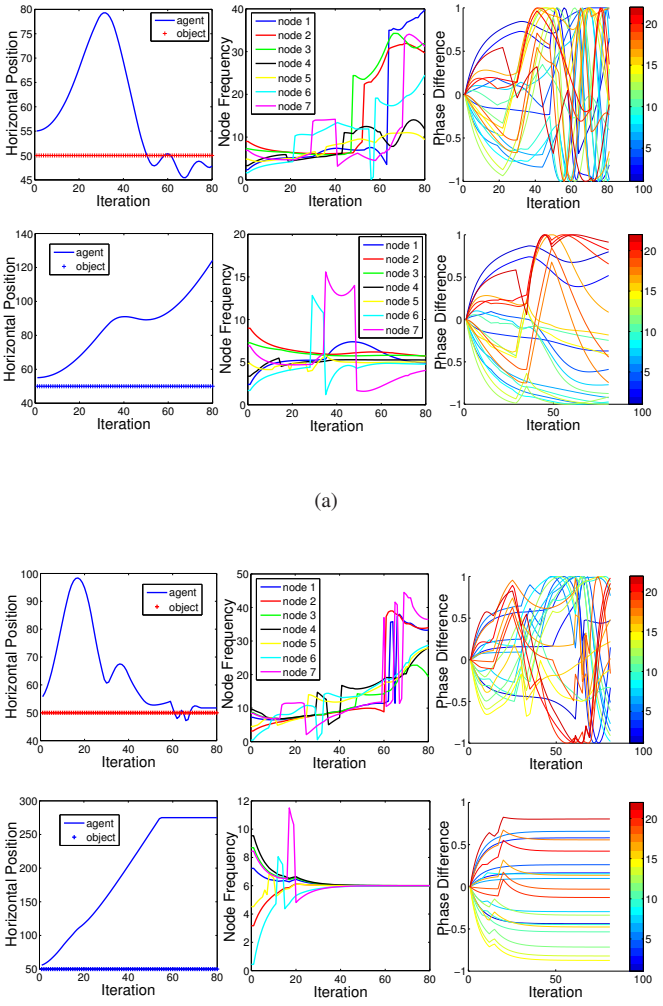

(a)

(b)

Fig. 4. Detailed behaviour of the agent's internal and external dynamics in Experiment 1 for the ring topology (a) and fully connected topology (b). The top three graphics refer to the circle catch behaviour and the bottom ones to the square avoidance behaviour. The leftmost illustrates the horizontal coordinate of the agent and the object, the middle one shows the frequency of each node of the network as the task progresses and the rightmost ones present the 21 ($C_{7,2}$) possible phase differences, calculated using Equation 3 (see text for details).

The following analysis will focus on the fully connected topology. The training fitness of the best evolved individual was 0.97 out of 1.00, and the generalization fitness over 100 aleatory runs was 0.92. Figure 3(b) illustrates the generalization test. Regarding the two architectures, the first comparison that can be made is that the fully connected topology presented a better performance in centring and

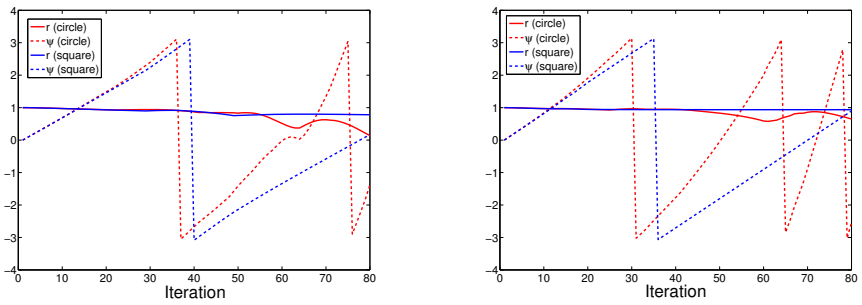

Fig. 6. Experiment 1 synchronisation index and the mean phase of the network for the ring topology (a) and the fully connected topology (b) , calculated according to Equation 2

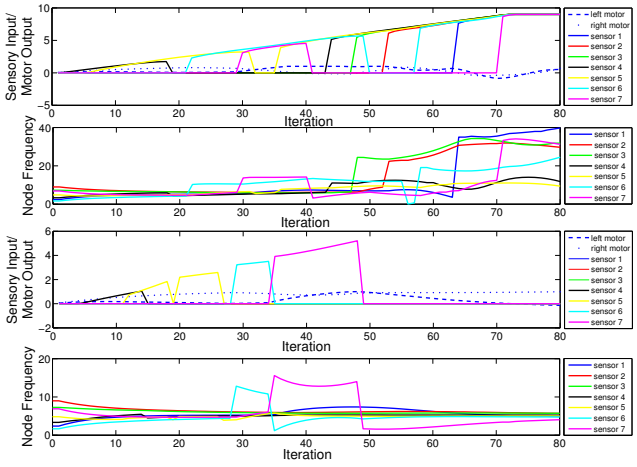

Fig. 5. Sensory input and the motor output, and the frequency of each node (upper two graphics refer to circle catch, bottom two for square avoidance, respectively) for the Experiment 1, ring topology case.

catching circles, but showed a poorer performance when the circles started in a relatively distant position from the robotic agent (note the poor catching behaviour when the initial horizontal separation is near the maximum value of 50).

In Figure 4(b), it is possible to observe that the frequency and phase dynamics for the circle catch behaviour (top 3 graphics of the figure) are similar to the ones observed in Figure 4(a) and analysed in the paragraphs above. However, the square avoidance behaviour, represented in the bottom three graphics of Figure 4(b), presents a noticeable different strategy. The robotic agent moves very fast to one side of the scenario (leftmost graphic), eventually not having its sensors stimulated by the square anymore. This lack of stimulus drives the system to a much more synchronized state than the one observed in the previous experiment, and a near-synchronous state is obtained with mean frequency of the order of $6rad/s$ (observe the middle graphic). As a consequence, the phase differences (shown in the rightmost part of the figure) become almost constant, and the robotic agent's motors speed, dictated by the phase differences and the output matrix W, stabilize in a constant value (leftmost graphic). Therefore, without external stimulus the network has an internal dynamics with all nodes oscillating near the same frequency. Internally generated brain activity, regardless of environmental inputs, is stressed by Engel et al. [5] as one of the key elements in cognitive processes. Figure 6(b) gives an overall picture of the synchronisation index and the mean phase of the network during the experiment, corroborating with the previous analysis.

B. Experiment 2

In the second experiment, the robotic agent is controlled by the fully connected network architecture, given its slightly better performance obtained in the previous experiment in the catching circles part of the task. Remember that the robot has to catch falling circles under normal and inverted vision.

Evolved robotic agents with good performance were obtained. The training fitness for the best evolved individual was 0.94 out of 1.00, and the generalization fitness over 100 random runs was 0.93. Figure 7 illustrates the generalisation test. For both scenarios, the adopted strategy seems to be: move to one side of the object (in this case the left side), where robotic agents with normal visual have their right sensors stimulated whereas robotic agents with inverted vision have their left sensors stimulated, and then centre in the object.

Looking at Figure 8 it is possible to see that the strategy for the normal and inverted vision tasks is almost the same, but the oscillatory activity of the network and its phase dynamics are quite different, illustrating the multiple roles a single oscillator can have in the network. For example, near iteration 60, in the normal vision scenario (upper part of the figure, middle graphic), the frequency of each node is varying and there is no apparent synchronisation. Near the same iteration, for the inverted vision case (bottom part of the figure), one can observe two almost synchronized clusters appearing: one formed by 4 nodes, the other formed by 2 nodes and the unsynchronized remaining node oscillating in a much higher frequency.

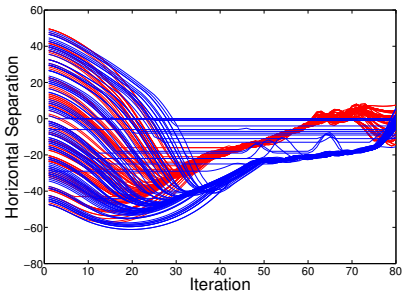

Fig. 7. The generalization performance of the agent over 100 aleatory runs in Experiment 2. The red colour is related to the normal vision case and the blue colour to the inverted vision scenario. The plot illustrates the value of the horizontal separation of the agent and the object along 80 iterations.

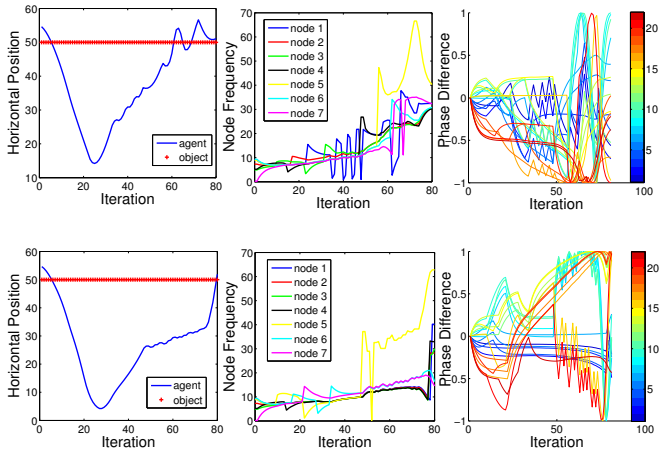

Fig. 8. Detailed behaviour of the agent's internal and external dynamics in Experiment 2. The leftmost illustrates the horizontal coordinate of the agent and the object, the middle one shows the frequency of each node of the network as the task progresses and the rightmost ones present the phase differences.

V. Discussion and Future Work

This work presents the first application of a widely used model of phase interacting oscillators, known as the Kuramoto model, to two different robotics tasks, which are commonly studied in minimally cognitive evolutionary robotics.

The first experiment, a categorical perception task, investigated the internal dynamics of the robotic agent, the synchronisation of the network and the resulting behaviour displayed by the robotic agent under two different network topologies, locally (ring shape) or fully connected. The experiment showed that nodes interact with each other and different synchronisation patterns can be obtained depending on the connectivity scheme, the environmental context and the internal state of system. A possible explanation for why the fully connected topology presents a higher synchronisation, compared to the ring topology, can be found in the work of Cumin and Unsworth [23], which indicates that increasing the connectivity of a network of oscillators increase their synchronisation. Also, Niebur et al. [35] state that a sparse coupling (i.e. few, possibly long-range connections) between oscillators are much more likely to promote synchronism than different coupling schemes such as nearest-neighbour or Gaussian distributed. This is not a trivial topic, as stressed by Wiley et al. [31], who mention the intractability and the importance of understanding the conditions under which a set of oscillators would synchronize. Understanding it could shed light into many different research areas, from the comprehension of the role of oscillatory properties in some diseases (e.g. Parkinson)[9] to the establishment of new parallel computing architectures [36].

The second experiment explored an inverted vision task where the robotic agent had to respond differently under the same sensory input conditions. It was possible to observe the different phase dynamics and the different synchronisation patterns of the nodes generating a very similar behaviour, illustrating the robotic agent's ability of tackling multiple and conflicting situations, even though the networks are composed of only 7 oscillatory nodes. All these observations relate to Buszaki [4] and Friston's [27] comments, which stress that the brain is not simply a reactive system responding to stimulus, but has spontaneous activity and interacts with the incoming sensory input, establishing dynamic cell assemblies by synchronizing and desynchronizing different groups of neurons.

We believe that exploring a simulated brain/body/environment system, in addition to the existing methods, could contribute to unveil important mechanisms of the neural system which may not be easily identifiable in living organisms and that could inspire the design of new robotic controllers. In this sense, the work presented in this paper devised a system that could eventually provide insights on the role of neuronal synchronisation and phase in the generation of cognitive behaviours, and to begin investigating the efficacy of such systems as practical robotic controllers.

There are many directions for future work, including: the study of different neural topologies for the network, including sparse connectivity schemes that would resemble with more fidelity the brain cortical structure; changing the coupling factor k so that it would vary depending on the activity and synchronisation level of different oscillators, adding flexibility to the neural assembly formation; compare the results obtained by large group, mean field neural approximation models, such as the one studied here, with models that focus on single neuron units; reproduce experiments with animals using an evolutionary robotics approach and observe if the results obtained could contribute somehow to the previous conclusions.

References

[1] B. Ermentrout. An adaptive model for synchrony in the firefly pteroptyx malaccae. *J. Math. Biol.*, 29:571–585, 1991.

[2] F. Hoppensteadt and E. Izhikevich. Synchronization of laser oscillators, associative memory, and optical neurocomputing. *Physical Review E*, 63(3), 2000.

[3] H. Berger. Uber das elektrenkephalogramm des menschen. *Arch. Psychiat. Nervenkr.*, 87:527–570, 1929.

[4] G. Buzsaki. *Rhythms of the Brain*. Oxford University Press, 2006.

[5] A.K. Engel, P. Fries, and W. Singer. Dynamic predictions: oscillations and synchrony in top-down processing. *Nat Rev Neurosci.*, 2(10):704–716, 2001.

[6] W. Singer. Neuronal synchrony: a versatile code for the definition of relations? *Neuron*, 24(1):49–65, 1999.

[7] P. Konig, A.K. Engel, and W. Singer. Integrator or coincidence detector? The role of the cortical neuron revisited. *Trends in Neurosciences*, 19:130–137, 1996.

[8] W. Singer. Synchronization of cortical activity and its putative role in information processing and learning. *Annual Review of Physiology*, 55:349–374, 1999.

[9] F. Varela, JP. Lachaux, E. Rodriguez, and J. Martinerie. The brainweb: phase synchronization and large-scale integration. *Nat. Rev. Neurosci.*, 2(4), 2001.

[10] Z. Li and J. Hopfield. Modeling the olfactory bulb and its neural oscillatory processings. *Biological Cybernetics, Springer Berlin/Heidelberg*, 61(5), 1989.

[11] E. Izhikevich. Weakly pulse-coupled oscillators, FM interactions, synchronization, and oscillatory associative memory. *IEEE Trans. Neural Networks*, 10(3):508–526, 1999.

[12] M. Kunyosi and L. Monteiro. Recognition of noisy images by PLL networks. *Signal Processing*, 89, 2009.

[13] R. Beer. The dynamics of active categorical perception in an evolved model agent. *Adaptive Behavior*, 11(4): 209–243, 2003.

[14] A.K. Seth, J.L. McKinstry, G.M. Edelman, and J.L. Krichmar. Visual binding through reentrant connectivity and dynamic synchronization in a brain-based device. *Cerebral Cortex*, 14, 2004.

[15] I. Harvey, E. Di Paolo, R. Wood, M. Quinn, and E. Tuci. Evolutionary robotics: a new scientific tool for studying cognition. *Artificial Life*, 11(1-2):79–98, 2005.

[16] D. Floreano, P. Husbands, and S. Nolfi. Evolutionary robotics. *In Siciliano and Khatib (Eds.) Springer Handbook of Robotics*, pages 1423–1451, 2005.

[17] D. Floreano and C. Mattiussi. *Bio-Inspired Artificial Intelligence*. MIT Press, 2008.

[18] A. Ijspeert, A. Crespi, D. Ryczko, and J.M. Cabelguen. From swimming to walking with a salamander robot driven by a spinal cord model. *Science*, 315(5817): 1416–1420, 2005.

[19] Y. Kuramoto. *Chemical Oscillation, Waves, and Turbulence*. Springer, New York, 1984.

[20] K. Dale and P. Husbands. The evolution of reaction-diffusion controllers for minimally cognitive agents. *Artificial Life*, 16, 2010.

[21] E. Izquierdo. *The dynamics of learning behaviour: a situated, embodied, and dynamical systems approach*. PhD thesis, Centre for Computational Neuroscience and Robotics, University of Sussex, 2006.

[22] E. A. Di Paolo. Homeostatic adaptation to inversion of the visual field and other sensorimotor disruptions. In *From Animals to Animats, SAB vol. 6, pp.440–449*. MIT Press, 2000.

[23] D Cumin and C Unsworth. Generalising the Kuramoto model for the study of neuronal synchronisation in the brain. *Physica D*, 226(2):181–196, 2007.

[24] G. Tononi, O. Sporns, and G. Edelman. Reentry and the problem of integrating multiple cortical areas: Simulation of dynamic integration in the visual system. *Cerebral Cortex*, 2:310–335, 1992.

[25] J. A. Acebrón, L. L. Bonilla, C. J. Pérez Vicente, F. Ritort, and R. Spigler. The Kuramoto model: A simple paradigm for synchronization phenomena. *Reviews of Modern Physics*, 77(1):137–185, 2005.

[26] C. Von der Malsburg. The correlation theory of the brain. *Internal report. Max-Planck-Institute for Biophysical Chemistry, Gottingen, Germany*, 1981.

[27] K. Friston. The labile brain. i. neuronal transients and nonlinear coupling. *Phil.Trans. R. Soc. Lond. B*, 355: 215–236, 2000.

[28] A. Winfree. *The geometry of biological time*. Springer-Verlag, 1980.

[29] K. Wiesenfeld, P. Colet, and S. Strogatz. Frequency locking in Josephson arrays: connection with the Kuramoto model. *Phys. Rev. E*, 57, 1998.

[30] L. Monteiro, N. Canto, and J. Orsatti, F.and Piqueira. Global and partial synchronism in phase-locked loop networks. *IEEE Transactions on Neural Networks*, 14(6), 2003.

[31] D. Wiley, S. Strogatz, and M. Girvan. The size of the sync basin. *Chaos*, 16, 2006.

[32] H. El-Nashar and H. Cerdeira. Determination of the critical coupling for oscillators in a ring. *Chaos*, 19(3), 2009.

[33] J. Schmidhuber, D. Wierstra, M. Galiolo, and F. Gomez. Training recurrent networks by Evolino. *Neural Comput.*, 19(3):757–779, 2007.

[34] P. Husbands, T. Smith, N. Jakobi, and M. O Shea. Better living through chemistry: Evolving GasNets for robot control. *Connection Science*, 10:185–210, 1998.

[35] E. Niebur, H. Schuster, D. Kammen, and C. Koch. Oscillator-phase coupling for different two-dimensional network connectivities. *Phys. Rev. A*, 44(10):6895–6904, 1991.

[36] G. Korniss, M. Novotny, H. Guclu, Z. Toroczkai, and P. Rikvold. Suppressing roughness of virtual times in parallel discrete-event simulations. *Science*, 299(677), 2003.